



Role of seepage forces on hydraulic fracturing and failure patterns

Alexander Rozhko

Thesis submitted for the degree of Philosophiae Doctor

Department of Physics University of Oslo, Norway

Thèse présentée pour obtenir le titre de docteur de

l'Université Joseph Fourier - Grenoble I - France

Spécialité: Sciences de la Terre et de l'Univers

Ph. D. committee:

Prof. Bjorn Jamtveit, Professor, University of Oslo

Prof. Steve Miller, Professor, University of Bonn

Prof. Chaouqi Misbah, Directeur de Recherche, University of Grenoble

September 2007

© Alexander Rozhko, 2007

*Series of dissertations submitted to the
Faculty of Mathematics and Natural Sciences, University of Oslo.*
No. 673

ISSN 1501-7710

All rights reserved. No part of this publication may be
reproduced or transmitted, in any form or by any means, without permission.

Cover: Inger Sandved Anfinsen.
Printed in Norway: AiT e-dit AS, Oslo, 2007.

Produced in co-operation with Unipub AS.
The thesis is produced by Unipub AS merely in connection with the
thesis defence. Kindly direct all inquiries regarding the thesis to the copyright
holder or the unit which grants the doctorate.

*Unipub AS is owned by
The University Foundation for Student Life (SiO)*

Preface

The work presented in this dissertation was conducted at the Department of Physics, University of Oslo in collaboration with the Department of Geosciences, Universite Joseph Fourier, Grenoble, during a period of three years.

I would like to thank my main supervisor, Professor Yuri Podladchikov, for shearing his knowledge, giving valuable criticism and inspiration. Many thanks to my second supervisor, Professor Francois Renard, for his advices, continuous encouragement and motivation. Special thanks to Dr. Galen Gisler for the proof reading and corrections of the scientific manuscripts.

Many thanks to Filip Nicolaisen and Christophe Calerne for being very nice officemates and friends. I am also very grateful towards all people who work and study at PGP for the rich scientific arguments and informal discussions.

During this work I was happy to receive a full financial support from PGP (Physics of Geological Processes), a Norwegian Center of Excellence at University of Oslo.

Finally, thanks to my wife Jana and son Ivan for their love, patience and support during my PhD education.

Alexander Rozhko

September 2007

Role of seepage forces on hydraulic fracturing and failure patterns

Abstract. The mechanical role of seepage forces on hydraulic fracturing and failure patterns was studied both by the analytical methods of the continuum mechanics and by numerical simulations. Seepage forces are frictional forces caused by gradients of pore-fluid pressure. Formation of different failure patterns (localized shear bands or tensile fractures) driven by the localized fluid overpressure in the poro-elasto-plastic medium was studied using a numerical code specially developed for this purpose. The pre-failure condition for different failure patterns and fluid pressure at the failure onset was predicted using a new analytical solution.

In the analytical solution the elliptical cavity filled with fluid in the non-hydrostatic far-field stress-state is considered. Since, the fluid pressure inside cavity differs from the far-field pore-fluid pressure; the poroelastic coupling is taking into account in the calculation of the deformation. Using Griffith's theory for failure and this analytical solution, the generalized equation for the effective stress law was obtained. This generalized effective stress law controls the failure in the fluid-saturated porous medium with a non-homogeneous fluid pressure distribution.

Rôle des forces de succion sur le mode de fracturation des roches en présence de fluides

Résumé. L'effet mécanique des forces de succion, forces exercées par un fluide qui se déplace dans un milieu poreux, a été étudié dans le cadre de la fracturation hydraulique des roches de la croûte terrestre. Cet effet a été étudié par des méthodes analytiques issues de la mécanique des milieux continus, et par des simulations numériques. Ces forces de succion sont des forces de frottement causées par des gradients de pression fluide dans les milieux poreux. Différents modes de fracturation (bandes de cisaillement localisées, fractures en mode I) causés par une augmentation localisée de la pression fluide dans la croûte ont été reproduits dans un milieu poro-élastique grâce à plusieurs codes numériques spécialement développés à cet effet. La valeur de la pression fluide lors de la nucléation de la fracturation est aussi prédite à l'aide d'une nouvelle solution analytique.

Dans la solution analytique, une cavité elliptique dans un solide poreux est remplie avec un fluide à une pression non-hydrostatique. On considère aussi que le milieu poreux est soumis à un champ de contrainte externe. Puisque la pression du

fluide dans la cavité est différente de la pression de pore dans la roche; le couplage poro-élastique est pris en compte dans le calcul des déformations. A partir de la théorie de Griffith qui donne une condition pour la propagation d'une fracture, et en utilisant la solution analytique obtenue, une équation généralisée a été obtenue pour la contrainte effective dans le milieu. Cette nouvelle loi décrit la fracturation dans un milieu poreux saturé avec un fluide, et dans lequel la distribution de pression fluide n'est pas homogène.

CONTENTS

Preface	i
Abstract	iii
Contents	v
Part I Theory	1
1. Introduction	3
2. Theoretical foundations	5
2.1 Poroelasticity and thermoelasticity	5
2.2 Pore-fluid pressure effect on deformation and failure	7
2.3 Failure envelope for rock	8
2.4 Poro-elasto-plasticity	9
2.5 Linear poro-elastic fracture mechanics	11
3. Summary of the papers	15
Resume of Paper I	15
Resume of Paper II	15
Resume of Paper III	16
Resume of Paper IV	17
Bibliography	19
Appendix The numerical modeling of the fluid flow in a porous elastoplastic medium (MatLab code)	21
Part II Scientific papers	31

Paper 1: Rozhko, A. Y., Y. Y. Podladchikov, and F. Renard (2007), Failure patterns caused by localized rise in pore-fluid overpressure and effective strength of rocks, *Geophys. Res. Lett.*, 34, L22304, doi:10.1029/2007GL031696.

Paper 2: A.Y. Rozhko, Role of seepage forces in faulting and earthquake triggering, *submitted to Tectonophysics*.

Paper 3: A.Y. Rozhko and Y.Y. Podladchikov, Role of fluid diffusion on failure and effective stress of porous solids, *in preparation*.

Paper 4: A.Y. Rozhko, Hydraulic fracturing of elliptical boreholes and stress measurements in a highly permeable poroelastic reservoirs, *in preparation*.

Scientific advisors:

Professor Yuri Podladchikov

Professor Francois Renard

Part I Theory

1. INTRODUCTION

In this dissertation I will study the role of *gradients of pore-fluid pressure* on the mechanical strength and failure patterns of the porous, fluid saturated materials. Mechanical role of *pore-fluid pressure* on the failure is well recognized nowadays in the literature, starting from the pioneering work of [Von Terzaghi \[1943\]](#), who demonstrated on the experimental ground that the failure of the fluid saturated porous material is controlled by the effective stress that is equal to the total stress minus fluid pressure. Later [Murrell \[1964\]](#) applied [Griffith's theory \[1920\]](#) to the elliptical crack, filled with fluid and demonstrated that Terzaghi's effective stress principle follows from Griffith's theory of failure. However, the mechanical role of *gradients of pore-fluid pressure* on failure is not well recognized. Since, it is common to assume that for any variation in pore-fluid pressure, the total stresses are constant. Such an assumption is not always warranted; because the gradients in pore-fluid overpressure create seepage forces and that these seepage forces modify the total stresses. The recent publications of [[Mourgues and Cobbold, 2003](#); [Cobbold and Rodrigues, 2007](#)] show the experimental evidence that the seepage forces have a strong effect on the initiation and direction of propagation for both shear and tensile fractures. In addition, there is a recent experimental evidence that the aftershocks can be triggered by the local decrease of the fluid pressure on the fault zone [[Miller et al, 2004](#)], these may be explained by the rise of seepage forces due to the pore-fluid pressure gradients.

Since most of the materials like rocks, soils, concretes and human bones are porous with a non-homogeneous fluid-pressure distribution, it is very important to understand the role of pore-fluid pressure gradients on the mechanical strength and possible failure patterns, developed during a mechanical failure. In this dissertation I made an attempt to improve the understanding of mechanical role of pore-fluid pressure gradients on failure. The investigation was conducted both by the analytical methods of the continuum mechanics and by numerical simulations. In order to study a possible failure patterns, driven by pore-fluid pressure gradients, I have developed two numerical codes (finite difference and finite element) that allowed me to model both tensile and shear fractures in porous elastoplastic medium. In order to predict the pre-failure condition I have developed two analytical solutions in which I calculated the seepage forces around the open and closed elliptical crack. These analytical solutions are developed using a Complex potentials method [[Muskhelishvili, 1977](#); [Timoshenko](#)

and Godier,1982] applied to the linear poroelastic medium [*Biot, 1941; Rice and Cleary, 1976*]. Applying a new analytical solution in the Griffith's theory of failure, I have found a new effective stress law that governs the failure in a porous solid with a non-homogeneous fluid pressure distribution.

The dissertation has two parts: the theory and the scientific manuscripts. In the first part of the thesis I briefly introduce the theoretical background in the context of the previous works, the overview of the literature and the main results of the thesis. In the appendix I present the numerical code which was developed to study the failure patterns. In the second part I analyze four scientific manuscripts, which reflect the main results of the thesis in details.

2. THEORETICAL BACKGROUND

The purpose for this chapter is to give a brief theoretical introduction to the scientific manuscripts presented in the second part of the thesis. More detailed description of the theory is better explained in the cited literature.

2.1 Poroelasticity and thermoelasticity

Governing equations

The poro-elastic model is an extension of linear elasticity that allows for and takes into account the presence of a diffusing pore fluid; it is relevant to the deformation and fracture of the porous elastic materials with applications to geophysics. The pore fluid is free to diffuse through the material and interact with the solid elastic skeleton. The diffusion process introduces the time dependence into the otherwise quasi-static elasticity equations. The poroelastic equations derived by Biot [1941], subsequently reformulated by Rice and Cleary [1976] are that the stress tensor σ_{ij} is given by

$$\sigma_{ij} = 2\mu\varepsilon_{ij} + 2\mu\varepsilon_{kk} \frac{\nu}{1-2\nu} \delta_{ij} + \alpha p_f \delta_{ij}, \quad (1)$$

where the repeated indices denote summation; the relation between the strain tensor ε_{ij} and the displacements u_i is $\varepsilon_{ij} = \frac{1}{2} \left(\frac{\partial u_i}{\partial x_j} + \frac{\partial u_j}{\partial x_i} \right)$; $\delta_{ij} = \begin{cases} 1 & \text{for } i = j \\ 0 & \text{for } i \neq j \end{cases}$ is the Kronecker delta (the positive compressive stress as a sign convention is used here).

According to equation (1) the deformation is controlled by the effective stress $\sigma'_{ij} = \sigma_{ij} + \alpha p_f \delta_{ij}$ [Garg and Nur, 1973], thus, the rheology relation for the effective stress can be formulated as follows

$$\sigma'_{ij} = \sigma_{ij} - \alpha p_f \delta_{ij} = 2\mu\varepsilon_{ij} + 2\mu\varepsilon_{kk} \frac{\nu}{1-2\nu} \delta_{ij}. \quad (1a)$$

The pore pressure p_f is related via

$$p_f = Q\zeta + \alpha Q\varepsilon_{kk} \quad (2)$$

to the variation of fluid volume content ζ , and the dilation, $e = \varepsilon_{kk}$. The constants and their physical interpretation are given in the next subsection. Provided there are no body

forces or fluid sources in the material the governing equations are written as the equilibrium equation for the stresses

$$\sum_j \frac{\partial}{\partial x_j} \sigma_{ij} = 0. \quad (3)$$

The force balance equation formulated for effective stress as follows

$$\sum_j \frac{\partial}{\partial x_j} \sigma'_{ij} = \alpha \frac{\partial}{\partial x_i} p_f. \quad (3a)$$

The term which appears on the right hand side in equation (3a) is commonly referred as *seepage force*. According to equation (3a) the physical meaning for seepage force is equivalent to the *volume force* which is acting along the gradients of the fluid pressure and equal to zero, when the fluid pressure is homogeneous, i.e. when the gradients are zero.

Darcy's law which relates mass flux to the gradient of pore pressure

$$q_i = -\rho_0 \kappa \frac{\partial}{\partial x_i} p_f, \quad (4)$$

and a mass-conservation equation for the pore fluid

$$\frac{\partial}{\partial t} m = -\frac{\partial}{\partial x_i} q_i, \quad (5)$$

where m is the mass of fluid per unit volume and ρ_0 is the reference density. Using equations (2, 4 and 5) the fluid diffusion equation for the pore pressure with a coupling term for the dilation can be written in the form:

$$\frac{\partial p_f}{\partial t} - \kappa Q \sum_j \frac{\partial^2 p_f}{\partial x_j^2} = \alpha Q \frac{\partial e}{\partial t}. \quad (6)$$

Poroelastic constants and their physical interpretation

The following symbolism is used in the previous subsection: α is the Biot-Willis poroelastic constant, that is, the ratio of fluid volume to the volume change of solid allowing the fluid to drain, where $0 \leq \alpha \leq 1$; μ is the shear modulus; ν, ν_u are drained and undrained Poisson ratios, where $0 \leq \nu \leq \nu_u \leq \frac{1}{2}$; κ is the permeability coefficient; $d\zeta / dp_f = 1/Q$ is a measure of the change in the fluid content generated in a unit reference volume during the change of the pressure with the strains kept constant,

where $Q = \frac{2\mu(v_u - \nu)}{\alpha^2(1-2\nu)(1-2\nu_u)}$ and $Q \geq 0$; and finally, ζ is the variation of fluid content per unit reference volume, i.e. mass of fluid per unit volume/initial density ρ_0 .

Similarity and difference between poro- and thermo- elasticity

The thermoelastic continuative equation is equivalent to the poroelastic continuative equation (1) if the fluid pressure p_f is changed to the temperature T ($p_f \rightarrow T$) and the Biot-Willis poroelastic constant is changed as follows $\alpha \rightarrow \frac{\alpha_T E}{1-2\nu}$, where α_T is the thermal expansion coefficient and E is a Young modulus [Rice and Cleary, 1976; Timoshenko and Goodier, 1982]. The difference between thermo and poro elasticity will appear in equation (6), i.e. the heat conduction equation is governed by equation

$$\frac{\partial T}{\partial t} - \kappa_h \sum_j \frac{\partial^2 p_f}{\partial x_j^2} = 0, \quad (7)$$

here κ_h is the heat conduction coefficient. In equation (7) the change in dilation does not contribute to the change in temperature. The seepage force in poroelastic equation (3a) is equivalent to the thermal stress in thermoelasticity.

Steady-state (quasi-static) poroelasticity

In case of a steady-state fluid filtration no time dependence is introduced to the fluid diffusion equation (6), which can be simplified to the ordinary Laplace equation as the following:

$$\sum_j \frac{\partial^2 p_f}{\partial x_j^2} = 0. \quad (8)$$

Now, as one can see from (6) and (7) in the case of the steady-state problems the poroelastic and thermoelastic equations are equivalent.

2.2 Pore-fluid pressure effect on deformation and failure

It is generally recognized that the pore-pressure has different effects on deformation and failure of the fluid saturated porous solid [Terzaghi, 1923; Skempton, 1961; Garg and Nur, 1973 Jaeger and Cook, 1979; Paterson and Wong, 2005]. Both the theoretical analysis and experimental observations show that, provided that the

rocks contain a connected system of pores, the failure is controlled by the Terzaghi effective stress σ''_{ij} defined as

$$\sigma''_{ij} = \sigma_{ij} - p_f \delta_{ij}. \quad (9)$$

However, the deformation is controlled by another effective stress law σ'_{ij} , formulated as follows

$$\sigma'_{ij} = \sigma_{ij} - \alpha p_f \delta_{ij}, \quad (10)$$

where σ_{ij} is the total stress tensor; p_f is the pore fluid pressure, α is the Biot-Willis coupling poroelastic constant (by convention, compressive stress is positive).

2.3 Failure envelope for rock

In nature, the rock failure occurs in two different modes: in the shear bands and in the tensile fractures. The laboratory triaxial experiments show that the Mohr-Coulomb criterion provides an accurate prediction for a shear failure [Jaeger and Cook, 1979; Paterson and Wong, 2005]:

$$\tau - \sigma''_m \sin(\phi) = C \cos(\phi), \quad (11)$$

where $\tau = \sqrt{\frac{(\sigma_{xx} - \sigma_{yy})^2}{4} + \sigma_{xy}^2}$ is the stress deviator, $\sigma''_m = \frac{\sigma_{xx} + \sigma_{yy}}{2} - p_f$ is the mean Terzaghi effective stress, C is the rock cohesion and ϕ is the internal friction angle.

On the other hand, Griffith's theory provides a theoretical criterion for tensile failure of a fluid-filled crack [Murrell, 1964]:

$$\tau - \sigma''_m = \sigma_T, \quad (12)$$

where σ_T is the tensile strength of the rock. This criterion has also been verified experimentally [Jaeger, 1963; Paterson and Wong, 2005].

Both the tensile and shear failure criteria are shown on the Mohr diagram (Figure 1), where lm is the Mohr-Coulomb envelope (eq. 11) and kl is the tensile cut-off limit (eq. 12). Any stress-state in a particular point of the solid can be shown by the Mohr circle on this diagram with radius τ and center σ''_m (τ and σ''_m are defined after equation (11)).

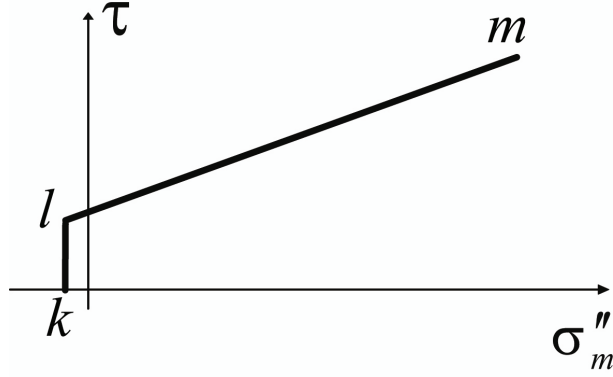


Figure 1. Failure envelope for rocks (lm is the Mohr-Coulomb envelope (eq. 11) and kl is the tensile cut-off limit (eq. 12)).

All Mohr-circles on the Mohr-diagram located below lm and on the right side of kl represent the stable combination of stresses in the elastic domain. However, if the Mohr circle touches the failure envelope klm , the solid undergoes the irreversible plastic deformation, which leads to the formation of shear bands and tensile fractures. Depending on the location of the circle touching the failure envelope, the formation of the shear bands (lm) or the tensile fractures (kl) takes place. The shear bands form at the angle of $\frac{\pi}{4} - \frac{\phi}{2}$ to the direction of maximum compressive (Terzaghi effective) stress; the tensile fractures develop perpendicularly to the direction of the maximum tensile (Terzaghi effective) stress.

2.4 Poro-elasto-plasticity

In physics and materials science plasticity is a property of a material to undergo a non-reversible deformation in response to an applied force. For many natural materials, the load applied to the sample will cause the deformation to behave in an elastic manner. Each increment of the load is accompanied by a proportional increment in extension, and when the load is removed, the piece returns exactly to its original size (Figure 2, blue line). However, once the load exceeds some threshold (described by equation (11) for shear loading and by equation (12) for tensile loading) the deformation increases more rapidly than in the elastic region (Figure 2, green curve), and when the load is removed, some amount of the extension remains. The further deformation of the material could lead to the fracture.

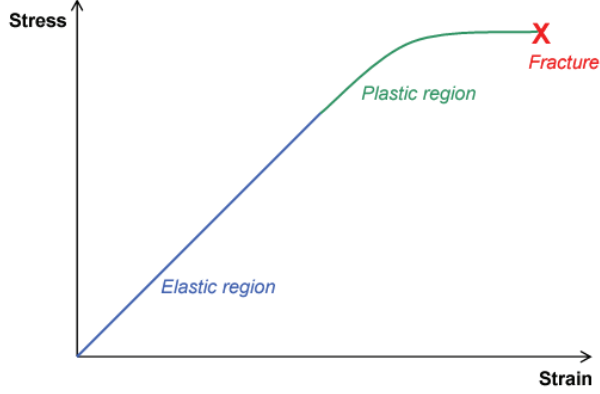


Figure 2. A stress-strain diagram. (The blue line shows the reversible elastic deformation domain, while the green curve shows the irreversible plastic deformation in the process zone, which accompanies the formation of the fracture.)

According to the general approach for poro-elasto-plastic deformation [Rice and Cleary, 1976; Vermeer, 1990], the full strain rate tensor is given by

$$\dot{\epsilon}_{ij} = \dot{\epsilon}_{ij}^{pe} + \dot{\epsilon}_{ij}^{pl} \quad (13)$$

where the superscripts *pe* and *pl* denote the poro-elastic and the plastic components, respectively. The poro-elastic strain rates can be written as:

$$\dot{\epsilon}_{ij}^{pe} = \frac{\dot{\sigma}_{ij} - \dot{\sigma}_m \delta_{ij}}{2G} + \frac{\dot{\sigma}_m - \alpha \dot{p}^f}{2G} \delta_{ij} \frac{1-2\nu}{1+\nu}. \quad (14)$$

The plastic strain rates are given by

$$\begin{aligned} \dot{\epsilon}_{ij}^{pl} &= 0 \text{ for } f < 0 \text{ or } (f = 0 \text{ and } \dot{f} < 0) \\ \dot{\epsilon}_{ij}^{pl} &= \lambda \frac{\partial q}{\partial \sigma_{ij}^n} \text{ for } f = 0 \text{ and } \dot{f} = 0 \end{aligned} \quad (15)$$

The yield function in the form $f = \max(f_{tension}, f_{shear})$, where $f_{tension}$ and f_{shear} are the yield functions for a failure in tension and in shear, respectively, defined as:

$$\begin{aligned} f_{tension} &= \tau - \sigma_m^n - \sigma_T \\ f_{shear} &= \tau - \sigma_m^n \sin(\phi) - C \cos(\phi) \end{aligned} \quad (16)$$

The parameter λ in (eq. 15) is the non-negative multiplier of the plastic loading [Vermeer, 1990], and q is the plastic flow function, defined as follows for a tensile (the associated flow rule) and shear failure (the non-associated flow rule):

$$\begin{aligned} q_{tension} &= \tau - \sigma_m'' \\ q_{shear} &= \tau - \sigma_m'' \sin(\nu) \end{aligned} \quad (17)$$

where ν is the dilation angle ($\nu < \phi$), that disappears after a few percent of strain. Note that in (eq. 14) the total stress is used, whereas the Terzaghi effective stress (eq. 9) applies in the failure equations (15-17).

Equations (13-17) along with (3, 8, 9) represent the full set of equations which governs a quasi-static propagation of the plastic deformations into either shear bands or tensile fractures (The numerical code which solves the system of equations is presented in the Appendix). The term tensile fracture is not used here in its classical sense as a discontinuity in both traction and displacement fields. Rather, it describes the inelastic material response in the process zone area that accompanies fracture onset and propagation [Ingraffea, 1987].

2.5. Linear elastic fracture mechanics

Fracture mechanics is the field of solid mechanics that deals with the behavior of the cracked bodies subjected to stresses and strains. The modern fracture mechanics is based on the Griffith's theory [1920], outlined below.

In order to explain why the experimental tensile strength of brittle materials is many times lower than the ultimate stress required for the breaking of the atomic bonds, Griffith [1920] proposed that the failure of materials may be controlled by the presence of small defects, which may propagate as cracks into the solid. This assumption was based on the work of Inglis who showed that the local stress at the tip of an elliptical crack can be concentrated many times higher than the macroscopic stress. Griffith proposed that the propagation requires the creation of the surface energy, which is supplied by the loss of the strain energy accompanying the relaxation of the local stresses as the crack advances. The failure occurs when the loss of the strain energy is sufficient to provide the increase in the surface energy.

The Griffith's theory was not accepted with proper attention for over twenty years both in Engineering and Academics communities. The consequences of the ignorance are devastating (Figure 3a), as for example, in order to estimate the strength of the structural constructions like ships, a simple beam theory (Figure 3b) was considered sufficient. The construction engineers measured the stresses in the various

parts of the hull with strain-gauges, and “proved” that simple beam theory gave results well inside the safety envelope of the materials. [Gordon, 1991].

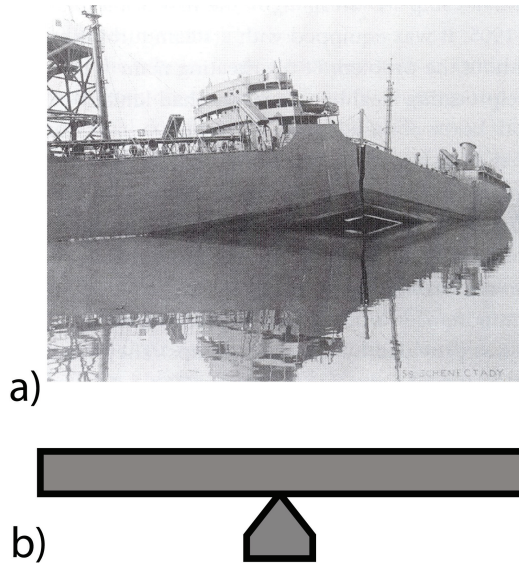


Figure 3a. Tanker SS Schenectady, fractured a day after its launch in January 1941.
Figure 3b. An elastic beam in the gravitation field was used as a standard method for calculating of ship’s strength.

Later in 1948, the naval research engineer Irwin formulated the Griffith’s theory in terms of stress concentrations rather than in terms of energy. Irwin introduced the *fracture toughness* concept which is universally accepted as the defining property of fracture mechanics. Irwin demonstrated that the Griffith’s theory can also be applied to ductile materials, provided that the size of the plastic zone located at the fracture tip is much smaller than the fracture length. Based on the Griffith’s theory, he represented the concept of a *strain-energy realize rate*, controlling the initiation and propagation of a fracture. Later in 1968 Rice introduced the *J-integral*, a method of calculation of the energy realized during a fracture propagation. This method is applicable for the materials with a generalized constitutive rheology, for example, for poro-elasto-plastic materials.

The Griffith’s energy criterion can be represented equivalently via the path-independent *J-integral* [Rice, 1968; Hellan, 1984]:

$$2\gamma \leq J, \tag{18}$$

here 2γ is the specific surface energy, assigned to one side of the fracture surface; and the path-independent J -integral is defined as:

$$J = \int_{\Gamma} [U dx_2 - \vec{T} \cdot \frac{\partial \vec{u}}{\partial x_1} ds], \quad (19)$$

here U is the strain energy density function, defined as [Atkinson and Craster, 1991; Wang, 2000]:

$$U = \frac{1}{2} \sigma_{ij} \varepsilon_{ij} + p_f \zeta, \quad (20)$$

where ζ is the variation of fluid content per unit reference volume, introduced in equation (2).

In equation (19) the integral is taken along any path Γ (counter-clockwise) around the crack tip; \vec{T} is the vector of traction on Γ , with components $T_i = \sigma_{ij} n_j$, n_j is the normal to the curve Γ ; s is the arc length along Γ . Since a path of integration can be arbitrary chosen in the poroelastic regime, the curve Γ can be taken from the lower side ($x_1 = a$, $x_2 = 0^-$), past ($x_1 = a + \Delta a$, $x_2 = 0$), to the upper side at ($x_1 = a$, $x_2 = 0^+$). Since $dx_2 = 0$, equation (19) becomes ([Rice, 1968; Hellan, 1984]):

$$J = \lim_{\Delta a \rightarrow 0} \frac{1}{2\Delta a} \int_a^{a+\Delta a} \sigma_{2i}(x_1, 0, a) [u_i(x_1, 0^+, a + \Delta a) - u_i(x_1, 0^-, a + \Delta a)] dx_1, \quad (21)$$

where $\sigma_{2i}(x_1, 0, a)$ is the stress on the crack tip of the length $2a$; $u_i(x_1, 0^\pm, a + \Delta a)$ are the displacements on the crack tip of the length $2(a + \Delta a)$ [Hellan, 1984].

3. SUMMARY OF THE PAPERS

A brief summary of the papers is presented in the following order. The results of the papers I and II are based on the new analytical solution derived for a closed crack, while in the papers III and IV, I derived the analytical solution for an open crack. Yuri Podladchikov introduced me to the numerical modeling which made me possible to develop my own numerical codes in order to study the failure patterns in the paper I. Both Yuri Podladchikov and Francois Renard helped me to formulate the problem for the first manuscript and improve the text. Yuri Podladchikov also helped me to formulate the problem for the third paper. Papers II and IV have a single author.

Resume of Paper I

In the first paper we have studied various failure patterns, driven by a localized fluid source at the depth. The reasons why the fluid pressure can be laterally localized at the depth in the earth's crust are reviewed in [*Hickman et al, 1995*]. There have been developed two numerical codes using a finite difference and finite element methods which allowed to model failure patterns caused by the tensile and/or shear failures in a porous elastoplastic medium [*Biot, 1941; Rice and Cleary, 1976; Vermeer and de Borst, 1984; Wang, 2000*]. It is demonstrated that at least five failure patterns (tensile or shear) can occur. Moreover, we calculate analytically the critical pressure at which a failure nucleates and we propose a phase-diagram of the failure patterns, illustrating the dependence on the model parameters. The results of the paper have a direct application to the geological problems, because many natural systems, such as magmatic dykes, mud volcanoes, hydrothermal vents, or fluid in faults, show the evidence that the pore pressure increase is localized instead of being homogeneously distributed. This paper contains animations in the Auxiliary Materials section, which illustrate the evolution of failure patterns during the increase of the pore-fluid pressure at the localized source.

Resume of Paper II

In the second paper we discuss the effects of the coupling between the deformation and pore-fluid diffusion on faulting and failure processes. We consider an arbitrarily oriented preexisting fault zone of finite length, located at the depth with a

given fluid overpressure in it and surrounded by the porous and permeable rocks. The intrinsic elastic and transport properties of these rocks are assumed to be isotropic and homogeneous. The seepage forces caused by the steady-state fluid diffusion from the fault zone to the surrounding permeable rocks are calculated analytically using the complex-potentials method for the pore-elasticity and conformal mapping. The pore-fluid overpressure required for the fault reactivation is calculated analytically in 2D, assuming that the tectonic stress state, the rock intrinsic properties and the geometry of the pre-existing fault are known. The solution is applied to the micro-earthquake triggering caused by the hydrocarbon withdrawals from a reservoir. Other applications such as the storage of carbon dioxide in porous rocks and geothermic exploitation are also considered.

Resume of Paper III

In the third paper we calculate explicitly a seepage forces caused by the coupling of pore-pressure gradients to the rock deformation. We apply the obtained analytical solution [[Auxiliary materials for paper 3](#)] to the Griffith's theory of failure and demonstrate that the failure is controlled by a *new effective stress law*:

$$\sigma_{\infty} + Wp_{\infty} + (1-W)p_c \geq T_0 = \sqrt{\frac{4\gamma\mu}{\pi a(1-\nu)}},$$

$$\text{with } W = \frac{\alpha}{2} \frac{1-2\nu}{1-\nu} \left(1 - \frac{1}{\ln \frac{2c}{a}}\right) \quad (22)$$

where σ_{∞} is the macroscopic far-field stress and T_0 is the theoretical tensile strength of the material, which depends on the length of preexisting crack a ; the specific surface energy γ required for the creation of a new fractured surface; the shear modulus μ ; and the Poisson ratio ν ; α is the Biot-Willis poroelastic constant [[Paterson and Wong, 2005](#)]; c is the size of a body containing a crack; p_{∞} is the far-field pore-fluid pressure and p_c is the crack fluid pressure.

According to equation (22), during the uniform rise of the pore fluid pressure inside the porous medium the onset of fracture growth is controlled by the remote Terzaghi's effective stress,

$$\sigma' = \sigma_{\infty} + p_{\infty}, \quad (23)$$

since the fracture pressure p_c at the onset of the fracture growth is equal to the pore pressure p_∞ in the surrounding fluid-saturated rock. The tensile strength decreases as the fracture grows in length. Therefore, the fracture is accelerated by an increase in a tensile excess load (and by the release of elastic strain energy), if the remote stress and the pore pressure are kept constant. In reality, however, the fracture pressure p_c in a propagating double-ended fracture does drop because the volume of the growing fracture increases. This causes an inflow of the pore-fluid from the surrounding rock at a rate depending on the hydraulic conductivity of the rock. At the same time, the decrease in fracture pressure will entail a decrease in the driving stress, which will retard, possibly stabilize, or even temporary stop the propagation of a tensile fracture inside the fluid saturated rock. Since the rocks in the earth's crust are mostly under a compressive stress state at the depth ($\sigma_\infty < 0$), the presence of fluid in the pores $p_\infty > 0$ could promote the propagation of fracture during an earthquake, which takes place when

$$\sigma'' = \sigma_\infty + Wp_\infty \geq 0. \quad (24)$$

Thus, the main result of this paper is the following: we demonstrate that the initiation of a tensile fracture is controlled by the Terzaghi's effective stress, while the propagation of a tensile fracture is controlled by the effective stress:

$$\sigma'' = \sigma_\infty + \frac{\alpha}{2} \frac{1-2\nu}{1-\nu} p_\infty. \quad (25)$$

Resume of Paper IV

In the forth paper we propose a hydraulic fracturing criterion for an elliptical cavity in a permeable poroelastic medium under a non-hydrostatic far-field stress state. The elliptical cavity is filled with a constant fluid pressure p_c inside the cavity. The far-field pore fluid pressure p_∞ is different from the fluid pressure in the cavity ($p_c \neq p_\infty$), therefore the fluid can infiltrate from the cavity into surrounding permeable rock. The diffusive fluid couples to the rock deformation, creating an additional stress field via seepage forces which has an additional effect on the initiation of a fracture. We considered the steady-state fluid flux from the cavity into a surrounding permeable reservoir with the homogeneous and isotropic intrinsic properties. We considered two applications of the analytical solution: the hydraulic fracturing of boreholes with an

elliptical cross-section and the *in situ* stress measurements in a highly permeable formation. We demonstrate that the small deviations of the borehole's cross-section from the circular have an additional effect on the *breakout pressure* and show that the *fluid leakage* has a strong influence on the fracture *closure pressure*. It is shown that if a reservoir is highly permeable than a fracture closure pressure is equal to

$$p_c = -\frac{\sigma_h + \eta p_\infty}{1 - \eta}, \quad (26)$$

where σ_h is the minimum *in situ* stress, p_∞ is the far-field pore pressure; $\eta = \frac{\alpha}{2} \frac{1 - 2\nu}{1 - \nu}$ here α is the Biot-Willis poroelastic constant and ν is the Poisson ratio. This formula shows that the poroelastic coupling must be taken into account in the highly permeable reservoirs, since nowadays it is assumed in industry that $p_c = -\sigma_h$.

BIBLIOGRAPHY

- Atkinson, C., Craster R.V. 1991. Plane strain fracture in Poroelastic Media. Proceedings: Mathematical and Physical Sciences, 434(1892), 605-633.
- Biot, M. A. 1941. General theory of three-dimensional consolidation. *Journal of Applied Physics* 12, 155-164.
- Cobbold, P.R., Rodrigues, N. 2007. Seepage forces, important factors in the formation of horizontal hydraulic fractures and bedding-parallel fibrous veins ('beef' and icone-in-cone). *Geofluids* 7 (3): 313-322.
- Garg, S. K., and Nur, A. 1973. Effective stress laws for fluid-saturated porous rocks. *Journal of Geophysical Research*, 78(26), 5911-5921.
- Gordon, J.E. 2006. *The New Science of Strong Materials or Why You Don't Fall through the Floor*. Princeton University Press. pp. 328.
- Griffith, A. A. 1920. The Phenomena of Rupture and Flow in Solids, *Phil. Trans. Roy. Soc., London*, A, 221, 163-198.
- Hellan, K. 1984. *Introduction to fracture mechanics*. McGraw-Hill, Inc., New York. 302 pp.
- Hickman, S., Sibson, R., Bruhn, R. 1995. Introduction to special section: Mechanical involvement of fluids in faulting. *Journal of Geophysical Research*, 100(B7), 12831-12840.
- Ingrafea, A. R. 1987. Theory of crack initiation and propagation in rock, in *Fracture Mechanics of Rock*, edited by B. K. Atkinson, pp. 71-110, Academic Press, London.
- Irwin, G. R. 1948 *Fracture of metals* (ed.F. Jonassen, W. B. Roop & R. T. Bayless),pp. 147-166. Cleveland, OH: ASM.
- Miller S. A., Collettini, C., Chiaraluce, L., Cocco, M., Barchi, M. and Kaus, B. 2004. Aftershocks driven by a high pressure CO₂ source at depth. *Nature*, 427, 724-727.
- Mourgues R., and Cobbold, P.R. 2003. Some tectonic consequences of fluid overpressures and seepage forces as demonstrated by sandbox modeling, *Tectonophysics*, 376, 75-97.
- Murrell, S. A. F. 1964. The theory of propagation of elliptical Griffith cracks under various conditions of plane strain or plain stress. Parts 2, 3; *British Journal of Applied Physics*, 15, 1211-23.

- Muskhelishvili, N.I. 1977. *Some Basic Problems in the Mathematical Theory of Elasticity*. Springer, Berlin. 768 pp.
- Paterson, M. S., and Wong, T.-F. 2005. *Experimental Rock Deformation-The Brittle Field*, 346 pp., Springer, Berlin.
- Rice, J. 1968. Mathematical analysis in the mechanics of fracture. In Liebowitz, H., editor, *Fracture - An advanced treatise*, volume 2, pages 191–311. Pergamon Press, Oxford.
- Rice, J. R., and Cleary, M. P. 1976. Some basic stress-diffusion solutions for fluid-saturated elastic porous media with compressible constituents. *Reviews of Geophysics and Space Physics*, 14, 227-241.
- Terzaghi, K. 1943. *Theoretical Soil Mechanics*, John Wiley and Sons, 528 pp., New York.
- Timoshenko, S. P., Goodier, J.N. 1982. *Theory of Elasticity*. McGraw-Hill, New York. 608 pp.
- Vermeer, P.A., de Borst, R. 1984. Non-associated plasticity for soils, concrete and rock. *Heron*, 29(3), 3-62.
- Wang, H.F. 2000. *Theory of Linear Poroelasticity with Applications to Geomechanics and Hydrology*. Princeton University Press, Princeton and Oxford. 276 pp.

APPENDIX: THE NUMERICAL MODELING OF THE FLUID FLOW IN A POROUS ELASTOPLASTIC MEDIUM (MatLab code)

In this appendix I will present an explicit finite difference MatLab code based on the Fast Lagrange Analysis of Continua, which I have developed during my PhD in order to model various failure patterns caused by the localized pore-pressure increase. The results of the modeling are presented in the first scientific manuscript. The animations that show the evolution of failure patterns during the localized increase of a fluid overpressure is presented in the Auxiliary materials for first paper.

The code consists of the main (calling) program: **Main.m** and five subroutines: **Pressure_Initialization.m**, **Pcrit.m**, **YieldFunction_array.m**, **YieldFunction_new.m** and **Plasticity.m**.

In order to run the code, all files must be located in the same folder. One should run **Main.m** program in MatLab.

Main.m

```
clear;
%physics
H = [4,1]; % Box size L and h
dH = H(2)/10; % Fluid source size w
ro_i = 1e8; % 'computational' density
phi = 35*pi/180; % friction angle
psi = 0*pi/180; % dilation angle
tan_phi = tan(phi);
sin_phi = sin(phi);
cos_phi = cos(phi);
sin_psi = sin(psi);
A = 0.2; % Sh=A*Sv
Earr = 2.6667e7; % Young modulus
nu = 0.3; %Poison ratio
K = Earr/3/(1 - 2*nu); % Bulk modulus
G = Earr/2/(1 + nu); % Shear modulus
kf = 0.4*1.05e6;
Vp = sqrt(max(9*K*G/(3*K+G))/ro_i); % Wave velos
Cohesion = 0.1; % Cohesion
St = Cohesion/8; % Tensile strength
%numerics
nx = [151,51]; % Resolution
dx = H./(nx-1); %
dt = 1/4*min(dx)/Vp/2; % Time step
damp = 1e-1; % 'Elastic' damper
time_out = 40;
% initialization
x = [0:dx(1):H(1)]';
y = [0:dx(2):H(2)];
x2D = repmat(x, [1, nx(2)]);
```

```

y2D      = repmat(y, [nx(1), 1]);
xc       = [dx(1)/2:dx(1):H(1)-dx(1)/2]';
yc       = [dx(2)/2:dx(2):H(2)-dx(2)/2];
x2Dc    = repmat(xc, [1, nx(2)-1]);
y2Dc    = repmat(yc, [nx(1)-1, 1]);
Pre_flu  = zeros(nx(1), nx(2)); % Fluid pressure
Pressure_Initialization; % Steady-state fluid pressure calculation
[Pc, Mode] = Pcrit(A, phi, Cohesion, St, H(2)/dH, nu); % Pc 'estimation'
Stress_check = zeros(3, nx(1)-1, nx(2)-1);
% F_plot    = zeros(nx(1)-1, nx(2)-1);
Size_S    = (nx(1)-1)*(nx(2)-1);
F         = -100*ones(nx(1)-1, nx(2)-1);
dStrain   = zeros(3, nx(1)-1, nx(2)-1);
% Terzaghi effective stress
Txy_eff   = zeros(nx(1)-1, nx(2)-1);
Syy_eff   = -(H(2)- y2Dc(:, :))*1/H(2);
Sxx_eff   = -A*(H(2)- y2Dc(:, :))*1/H(2);
% Total stress
Txy_tot   = zeros(nx(1)+1, nx(2)+1);
Syy_tot   = zeros(nx(1)+1, nx(2)+1);
Sxx_tot   = zeros(nx(1)+1, nx(2)+1);

Vx        = zeros(nx(1), nx(2)); %Solid velocity
Vy        = zeros(nx(1), nx(2));
Ux        = Vx;
Uy        = Vy;
time = 0;

Pre_flu_cen0 = (Pre_flu(1:end-1, 1:end-1) + Pre_flu(2:end, 1:end-1)...
+ Pre_flu(1:end-1, 2:end) + Pre_flu(2:end, 2:end))/4;
F_old      = -100;
while time < time_out
    time = time + dt;
    if time <= time_out % increase of pore pressure
        Pcoef = 0.9*Pc+8*Pc*time/time_out;
    end
    % Total stresses
    Pre_flu_cen = Pcoef*Pre_flu_cen0; % increase of pore
pressure
    Sxx_tot(2:end-1, 2:end-1) = (Sxx_eff - Pre_flu_cen);
    Syy_tot(2:end-1, 2:end-1) = (Syy_eff - Pre_flu_cen);
    Txy_tot(2:end-1, 2:end-1) = (Txy_eff);
    % Boundary conditions for total stress
    Syy_tot(:, end) = (1- y2Dc(1, end)/H(2)); % Top
    Txy_tot(:, end) = 0; % Top
    Sxx_tot(:, end) = A*(1- y2Dc(1, end)/H(2)); % Top

    Syy_tot(:, 1) = Syy_tot(:, 2); % Bottom
    Txy_tot(:, 1) = -Txy_tot(:, 2); % Bottom
    Sxx_tot(:, 1) = Sxx_tot(:, 2); % Bottom

    Syy_tot(1, :) = Syy_tot(2, :); % Right
    Txy_tot(1, :) = -Txy_tot(2, :); % Right
    Sxx_tot(1, :) = Sxx_tot(2, :); % Right

    Syy_tot(end, :) = Syy_tot(end-1, :); % Left
    Txy_tot(end, :) = -Txy_tot(end-1, :); % Left
    Sxx_tot(end, :) = Sxx_tot(end-1, :); % Left
    % VELOCITY UPDATE
    D_Sxx_x = (diff(Sxx_tot(:, 1:end-1), 1, 1) + ...

```



```

    diff(Sxx_tot(:,2:end),1,1))/dx(1)/2;
D_Txy_x = (diff(Txy_tot(:,1:end-1),1,1) + ...
    diff(Txy_tot(:,2:end),1,1))/dx(1)/2;
D_Txy_y = (diff(Txy_tot(1:end-1,:),1,2) + ...
    diff(Txy_tot(2:end,:),1,2))/dx(2)/2;
D_Syy_y = (diff(Syy_tot(1:end-1,:),1,2) + ...
    diff(Syy_tot(2:end,:),1,2))/dx(2)/2;

Vx      = Vx*(1-damp) + dt*(D_Sxx_x+D_Txy_y)/ro_i;
Vy      = Vy*(1-damp) + dt*(D_Txy_x+D_Syy_y-1)/ro_i;
% The Boundary Conditions for VELOCITY
Vx( 1,:) = 0;           %left x
Vx(end,:) = 0;         % right x
Vy(:,1)   = 0;         % Down Y
% Strains
dVx_dx    = (diff(Vx(:,1:end-1),1,1) + ...
    diff(Vx(:,2:end),1,1))/dx(1)/2;
dVy_dx    = (diff(Vy(:,1:end-1),1,1) + ...
    diff(Vy(:,2:end),1,1))/dx(1)/2;
dVx_dy    = (diff(Vx(1:end-1,:),1,2) + ...
    diff(Vx(2:end,:),1,2))/dx(2)/2;
dVy_dy    = (diff(Vy(1:end-1,:),1,2) + ...
    diff(Vy(2:end,:),1,2))/dx(2)/2;

dStrain(:) = [dVx_dx(:) dVy_dy(:) dVy_dx(:)+dVx_dy(:)'];
% Penalty stress
Stress_check(1,(:, :)) = Sxx_eff + dt * Earr/(1-2*nu)/(1+nu) * ...
    ((1-nu)*dVx_dx + nu.*dVy_dy);
Stress_check(2,(:, :)) = Syy_eff + dt * Earr/(1-2*nu)/(1+nu) * ...
    ((1-nu)*dVy_dy + nu.*dVx_dx);
Stress_check(3,(:, :)) = Txy_eff + dt * Earr/(1-2*nu)/(1+nu) * ...
    (1/2-nu) * (dVx_dy + dVy_dx);

% Plastic failure search
[F(:)]=YieldFunction_array(Size_S,Stress_check,phi,Cohesion,St);
ij = find(F<0);
% Elastic update
Sxx_eff(ij) = Stress_check(1,ij);
Syy_eff(ij) = Stress_check(2,ij);
Txy_eff(ij) = Stress_check(3,ij);
%
if max(F(:))>=0
    damp=0;
end
% Plastic update
Plasticity;
% Displacement
Ux = Ux + dt*Vx;
Uy= Uy + dt*Vy;
% Graphycs
if mod(round(time/dt),400)==400-1
    damp
    %Calculation of the strain deviator
    ex= diff(Ux,1,1);
    Ex = (ex(:,2:end)+ex(:,1:end-1))/2;
    ey= diff(Uy,1,2);
    Ey = (ey(2:end,:)+ey(1:end-1,:))/2;
    g1 = diff(Uy,1,1); G1 = (g1(:,2:end)+g1(:,1:end-1))/2;
    g2 = diff(Ux,1,2); G2 = (g2(2:end,:)+g2(1:end-1,:))/2;
    g = (G1+G2)/2;
    SI= sqrt((Ex-Ey).^2/4+g.^2); % Strain deviator

```

```

subplot(211), contour(x2Dc,y2Dc,SI,7), axis equal,
axis tight, axis off, shading interp, colorbar
subplot(212), pcolor(x2Dc,y2Dc,Syy_eff), axis equal,
axis tight, axis off, shading interp, colorbar
time
drawnow
end
end
% END OF Main.m

```

Pressure_Initialization.m

```

% fluid pressure initialization
nn      = prod(nx);
BM      = sparse(nn,nn);
nbcup   = zeros(nn,1);
nbclr   = zeros(nn,1);
nbcD    = zeros(nn,1);
ij2g    = reshape(1:nn,nx);
NNN=reshape(ij2g(2:end-1,2:end-1),1,[])*(1+nn)-nn;

BM(NNN)      = 1/dt + 2*kf/dx(1)^2+2*kf/dx(2)^2;
BM(NNN+nn)   = -kf/dx(1)^2;
BM(NNN-nn)   = -kf/dx(1)^2;
BM(NNN+nn*nx(1)) = -kf/dx(2)^2;
BM(NNN-nn*nx(1)) = -kf/dx(2)^2;
for i = 1:nx(1)
    neqn = ij2g(i,nx(2));
    BM(neqn,neqn) = 1;nbcup(neqn) = 1;
end
for j=1:nx(2)
    neqn = ij2g(1,j); BM(neqn,:) = 0; BM(neqn,neqn) = 1;
nbcclr(neqn) = 1;
    BM(neqn,ij2g(2,j)) = -1;
    neqn = ij2g(nx(1),j); BM(neqn,:) = 0; BM(neqn,neqn) = 1;
nbcclr(neqn) = 1;
    BM(neqn,ij2g(nx(1)-1,j)) = -1;
end
for i=1:nx(1)
    if (x(i)>=(H(1)-dH)/2)&(x(i)<=(H(1)+dH)/2)
        neqn = ij2g(i,1);
        BM(neqn,:) = 0;
        BM(neqn,neqn) = 1; nbcD(neqn) = 1;
    else
        neqn = ij2g(i,1); BM(neqn,:) = 0; BM(neqn,neqn)
= 1; nbcD(neqn) = 2;
        BM(neqn,ij2g(i,2)) = -1;
    end
end
Rhs      = zeros(nn,1);
Rhs(nbcD==1) = 1;
Rhs(nbcD==2) = 0;
Rhs(nbcup==0&nbcD==0&nbclr==0) =
Pre_flu(nbcup==0&nbcD==0&nbclr==0)/dt;
Pre_flu(:) = sparse(BM)\Rhs;
clear BM, clear Rhs, clear NNN
% END OF Pressure_Initialization

```

Pcrit.m

```

function [Pc,Mode]=Pcrit(A,phi,C,St,rhos,nu)
eta = (1-2*nu)/(1-nu)/2;
d1 = 1-eta+eta/log(2*rhos)/2;
d2 = eta/log(2*rhos)/2;
Sv = -1;
Delta = -(1-A);
po = [C*cos(phi)/(d1*sin(phi)+d2) C*cos(phi)/(d1*sin(phi)-d2)
St/(d1+d2) St/(d1-d2) St*log(2*rhos)/eta];
av = [ -sin(phi)/(d1*sin(phi)+d2) -sin(phi)/(d1*sin(phi)-d2)
-1/(d1+d2) -1/(d1-d2) 0];
ad = [(-1+sin(phi))/(d1*sin(phi)+d2)/2 (1+sin(phi))/(d1*sin(phi)-
d2)/2 0 1/(d1-d2) 0];
Pcarr = (po+av*Sv+ad*Delta)
Pc = min(Pcarr(Pcarr>0)); % Failure mode
Mode = find(Pcarr==Pc); % Failure pattern
% END OF Pcrit.m

```

YieldFunction_array.m

```

function [Ft]=YieldFunction_array(Size_S,Stress,phi,cohesion,St)
% This function search for elastic/plastic elements
Ft = -1000*ones(1,Size_S);
Ft1 = -1000*ones(1,Size_S);
Ft2 = -1000*ones(1,Size_S);
Mean_Stress = zeros(1,Size_S);
Mean_Stress(1,:) = (Stress(1,:)+Stress(2,:))/2; %Mean stress
TTau = zeros(1,Size_S); % Stress deviator
TTau(1,:) = (1/4*(Stress(1,:)-Stress(2,:)).^2+Stress(3,:).^2);
Ft1 = TTau - (Mean_Stress*sin(phi)-cohesion*cos(phi)).^2;
Ft2 = TTau - (Mean_Stress - St).^2;
Ft = max(Ft1,Ft2);
% END OF YieldFunction_array.m

```

YieldFunction_new.m

```

function [F,dFds,dQds]=...
    YieldFunction_new(Size_ij,Stress,phi,psi,cohesion,St)
F = -10*ones(1,Size_ij);
F1 = -10*ones(1,Size_ij);
F2 = -10*ones(1,Size_ij);
Mean_Stress = zeros(1,Size_ij);
Mean_Stress(1,:) = (Stress(1,:)+Stress(2,:))/2;
tau = zeros(1,Size_ij); % Stress deviator
tau(1,:) = (1/4*(Stress(1,:)-
Stress(2,:)).^2+Stress(3,:).^2).^(1/2);
% Partial derivative of yield function
dFds = zeros(3,Size_ij);
% Partial derivative of flow function
dQds = zeros(3,Size_ij);
% Yield function for tensile failure
F1 = tau + Mean_Stress-St;
% Yield function for shear failure
F2 = tau + Mean_Stress*sin(phi)-cohesion*cos(phi);
Mode2 = find(F2 > F1); % shear
Mode1 = find(F2 <= F1); % open

if size(Mode2,1)*size(Mode2,2)>0
    F(1,Mode2) = tau(1,Mode2) + ...

```

```

        Mean_Stress(1,Mode2)*sin(phi)-cohesion*cos(phi);
A2= 1/2*(Stress(1,Mode2)-Stress(2,Mode2))./(2*tau(1,Mode2));
B2 = Stress(3,Mode2)./tau(1,Mode2);

dFds(1,Mode2) = A2+1/2*sin(phi);
dFds(2,Mode2) = -A2+1/2*sin(phi);
dFds(3,Mode2) = B2;

dQds(1,Mode2) = A2+1/2*sin(psi);
dQds(2,Mode2) = -A2+1/2*sin(psi);
dQds(3,Mode2) = B2;
end
if size(Model,1)*size(Model,2)>0

F(1,Model) = tau(1,Model) + Mean_Stress(1,Model) - St;
A3 = 1/2*(Stress(1,Model)-Stress(2,Model))./(2*tau(1,Model));
B3 = Stress(3,Model)./tau(1,Model);
dFds(1,Model) = A3+1/2*sin(pi/2);
dFds(2,Model) = -A3+1/2*sin(pi/2);
dFds(3,Model) = B3;

angle = pi/2;
dQds(1,Model) = A3+1/2*sin(angle);
dQds(2,Model) = -A3+1/2*sin(angle);
dQds(3,Model) = B3;
end
% END OF YieldFunction_new.m

```

Plasticity.m

```

ij = find(F>=0);
Size_ij = length(ij);
if (Size_ij>0)

    if size(ij,1)~=Size_ij
        error('size error')
    end
    Stress=zeros(3,Size_ij);
    Stress(1,:)=Sxx_eff(ij);
    Stress(2,:)=Syy_eff(ij);
    Stress(3,:)=Txy_eff(ij);

    Strain = dStrain(:,ij);
    %Rheology matrix (Mat of coeff before str rate)
    D = zeros(3,3,Size_ij);
    FF = zeros(3,Size_ij);
    [F_old ,dFds,dQds] = YieldFunction_new(Size_ij,...
        Stress,phi,psi,Cohesion,St);
    % Elastoplastic Rheology

D(1,1,:) = G * (4 * dFds(3,:) .* G .* dQds(3,:) + 12 .* ...
dFds(2,:) .* K .* dQds(2,:) + 4 .* dFds(2,:) .* G .* ...
dQds(2,:) + 3 .* K .* dFds(3,:) .* dQds(3,:)) ./...
(3 .* dFds(3,:) .* G .* dQds(3,:) + 4 .* dFds(1,:) ...
.* G .* dQds(1,:) - 2 .* dFds(1,:) .* G .* dQds(2,:))...
+ 3 .* dFds(1,:) .* K .* dQds(1,:) +...
3 .* dFds(1,:) .* K .* dQds(2,:) + ...
3 .* dFds(2,:) .* K .* dQds(1,:) +...

```

```

3 .* dFds(2,:) .* K .* dQds(2,)- ...
2 .* dFds(2,:) .* G .* dQds(1,)+...
4 .* dFds(2,:) .* G .* dQds(2,));

D(2,1,:) = - G * (-3 * K * dFds(3,:) .* dQds(3,)+...
12 .* dFds(2,:) .* K .* dQds(1,)+ 4 .* dFds(2,)...
.* G .* dQds(1,)+ 2 .* dFds(3,).* G .* dQds(3,)) ./...
(4 .* dFds(1,).* G .* dQds(1,)- 2 .* dFds(1,).* ...
G .* dQds(2,)+ 3 .* dFds(1,).* K .* dQds(1,)+...
3 .* dFds(1,).* K .* dQds(2,)- 2 .* dFds(2,).* ...
G .* dQds(1,)+ 4 .* dFds(2,).* G .* dQds(2,)+...
3 .* dFds(2,).* K .* dQds(1,)+ 3 .* dFds(2,).* ...
K .* dQds(2,)+ 3 .* dFds(3,).* G .* dQds(3,));

D(3,1,:) = -dFds(3,).* G .* (4 .* G .* dQds(1,)- ...
2 .* G .* dQds(2,)+ 3 .* K .* dQds(1,)+ 3 .* ...
K .* dQds(2,)) ./ (4 .* dFds(1,).* G .* dQds(1,))...
- 2 .* dFds(1,).* G .* dQds(2,)+ 3 .* dFds(1,).* ...
K .* dQds(1,)+ 3 .* dFds(1,).* K .* dQds(2,)-...
2 .* dFds(2,).* G .* dQds(1,)+ 4 .* dFds(2,).* ...
G .* dQds(2,)+ 3 .* dFds(2,).* K .* dQds(1,)+ ...
3 .* dFds(2,).* K .* dQds(2,)+ ...
3 .* dFds(3,).* G .* dQds(3,));

D(1,2,:) = - G .* (4 .* dFds(1,).* G .* dQds(2,)+...
12 .* dFds(1,).* K .* dQds(2,)+ 2 .* dFds(3,).* ...
G .* dQds(3,)- 3 .* K .* dFds(3,).* dQds(3,)) ./...
(4 .* dFds(1,).* G .* dQds(1,)- 2 .* dFds(1,).* ...
G .* dQds(2,)+ 3 .* dFds(1,).* K .* dQds(1,)+ ...
3 .* dFds(1,).* K .* dQds(2,)- 2 .* dFds(2,).* ...
G .* dQds(1,)+ 4 .* dFds(2,).* G .* dQds(2,)+ ...
3 .* dFds(2,).* K .* dQds(1,)+ 3 .* dFds(2,).* ...
K .* dQds(2,)+ 3 .* dFds(3,).* G .* dQds(3,));

D(2,2,:) = G .* (3 .* K .* dFds(3,).* dQds(3,)+ ...
4 .* dFds(1,).* G .* dQds(1,)+ 12 .* dFds(1,).* ...
K .* dQds(1,)+ 4 .* dFds(3,).* G .* dQds(3,)) ./ ...
(4 .* dFds(1,).* G .* dQds(1,)- 2 .* dFds(1,).* ...
G .* dQds(2,)+ 3 .* dFds(1,).* K .* dQds(1,)+ ...
3 .* dFds(1,).* K .* dQds(2,)- 2 .* dFds(2,).* G .* ...
dQds(1,)+ 4 .* dFds(2,).* G .* dQds(2,)+ ...
3 .* dFds(2,).* K .* dQds(1,)+ 3 .* dFds(2,).* ...
K .* dQds(2,)+ 3 .* dFds(3,).* G .* dQds(3,));

D(3,2,:) = -dFds(3,).* G .* (3 .* K .* dQds(2,)- ...
2 .* G .* dQds(1,)+ 4 .* G .* dQds(2,)+ 3 .* ...
K .* dQds(1,)) ./ (4 .* dFds(1,).* G .* dQds(1,)) ...
- 2 .* dFds(1,).* G .* dQds(2,)+ 3 .* dFds(1,).* ...
.* K .* dQds(1,)+ 3 .* dFds(1,).* K .* dQds(2,))...
- 2 .* dFds(2,).* G .* dQds(1,)+ 4 .* dFds(2,).* ...
.* G .* dQds(2,)+ 3 .* dFds(2,).* K .* dQds(1,)+...
3 .* dFds(2,).* K .* dQds(2,)+...
3 .* dFds(3,).* G .* dQds(3,));

D(1,3,:) = -dQds(3,).* G .* (4 .* dFds(1,).* G...
- 2 .* dFds(2,).* G + 3 .* dFds(2,).* K +...
3 .* dFds(1,).* K) ./ (4 .* dFds(1,).* ...
G .* dQds(1,)- 2 .* dFds(1,).* G .* dQds(2,))...
+ 3 .* dFds(1,).* K .* dQds(1,)+ 3 .* dFds(1,).* ...
.* K .* dQds(2,)- 2 .* dFds(2,).* G .* dQds(1,)+ ...

```

```

4 .* dFds(2,:) .* G .* dQds(2,:) + 3 .* dFds(2,:) .*...
K .* dQds(1,:) + 3 .* dFds(2,:) .* K .* dQds(2,:)...
+ 3 .* dFds(3,:) .* G .* dQds(3,:));

D(2,3,:) = -dQds(3,:) .* G .* (-2 .* dFds(1,:) .* G ...
+ 4 .* dFds(2,:) .* G + 3 .* dFds(2,:) .* K + 3 .*...
dFds(1,:) .* K) ./ (4 .* dFds(1,:) .* G .* dQds(1,:)...
- 2 .* dFds(1,:) .* G .* dQds(2,:) + 3 .* dFds(1,:)...
.* K .* dQds(1,:) + 3 .* dFds(1,:) .* K .* dQds(2,:)...
- 2 .* dFds(2,:) .* G .* dQds(1,:) + 4 .* dFds(2,:) .*...
G .* dQds(2,:) + 3 .* dFds(2,:) .* K .* dQds(1,:) +...
3 .* dFds(2,:) .* K .* dQds(2,:)...
+ 3 .* dFds(3,:) .* G .* dQds(3,:));

D(3,3,:) = G .* (4 .* dFds(1,:) .* G .* dQds(1,:)...
- 2 .* dFds(1,:) .* G .* dQds(2,:) - 2 .* dFds(2,:)...
.* G .* dQds(1,:) + 4 .* dFds(2,:) .* G .* dQds(2,:) +...
3 .* dFds(1,:) .* K .* dQds(1,:) + 3 .* dFds(1,:)...
.* K .* dQds(2,:) + 3 .* dFds(2,:) .* K .* dQds(1,:)...
+ 3 .* dFds(2,:) .* K .* dQds(2,:)) ./ (4 .* dFds(1,:)...
.* G .* dQds(1,:) - 2 .* dFds(1,:) .* G .* dQds(2,:) +...
3 .* dFds(1,:) .* K .* dQds(1,:) + 3 .* dFds(1,:)...
.* K .* dQds(2,:) - 2 .* dFds(2,:) .* G .* dQds(1,:)...
+ 4 .* dFds(2,:) .* G .* dQds(2,:) + 3 .* dFds(2,:)...
.* K .* dQds(1,:) + 3 .* dFds(2,:) .* K .* dQds(2,:)...
+ 3 .* dFds(3,:) .* G .* dQds(3,:));

FF(1,:) = -(-2 .* G .* dQds(2,:) + 4 .* G .* dQds(1,:) ...
+ 3 .* K .* dQds(2,:) + 3 .* K .* dQds(1,:)) ./...
(4 .* dFds(1,:) .* G .* dQds(1,:) - 2 .* dFds(1,:)...
.* G .* dQds(2,:) + 3 .* dFds(1,:) .* K .* dQds(1,:) + ...
3 .* dFds(3,:) .* G .* dQds(3,:) + 3 .* dFds(1,:) .*...
K .* dQds(2,:) + 3 .* dFds(2,:) .* K .* dQds(1,:)...
+ 3 .* dFds(2,:) .* K .* dQds(2,:) - 2 .* dFds(2,:) .*...
G .* dQds(1,:) + 4 .* dFds(2,:) .* G .* dQds(2,:));

FF(2,:) = -(4 .* G .* dQds(2,:) - 2 .* G .* dQds(1,:) +...
3 .* K .* dQds(2,:) + 3 .* K .* dQds(1,:)) ./ (4 .*...
dFds(1,:) .* G .* dQds(1,:) - 2 .* dFds(1,:) .* ...
.* G .* dQds(2,:) + 3 .* dFds(1,:) .* K .* dQds(1,:) + ...
3 .* dFds(3,:) .* G .* dQds(3,:) + 3 .* dFds(1,:)...
.* K .* dQds(2,:) + 3 .* dFds(2,:) .* K .* dQds(1,:)...
+ 3 .* dFds(2,:) .* K .* dQds(2,:) - 2 .* dFds(2,:)...
.* G .* dQds(1,:) + 4 .* dFds(2,:) .* G .* dQds(2,:));

FF(3,:) = -3 .* G .* dQds(3,:) ./ (4 .* dFds(1,:) .*...
G .* dQds(1,:) - 2 .* dFds(1,:) .* G .* dQds(2,:)...
+ 3 .* dFds(1,:) .* K .* dQds(1,:) + 3 .* dFds(3,:)...
.* G .* dQds(3,:) + 3 .* dFds(1,:) .* K .* dQds(2,:) + ...
3 .* dFds(2,:) .* K .* dQds(1,:) + 3 .* dFds(2,:)...
.* K .* dQds(2,:) - 2 .* dFds(2,:) .* G .* dQds(1,:)...
+ 4 .* dFds(2,:) .* G .* dQds(2,:));

%*****
Stress = dt*shiftdim(sum(reshape(reshape(D, ...
[9, Size_ij]).*repmat(Strain,3,1), [3,3,Size_ij]),1)...
+ Stress + [[FF(1,:).*F_old(1,)];...
[FF(2,:).*F_old(1,)]; [FF(3,:).*F_old(1,)]]);

Sxx_eff(ij) = Stress(1,:);

```

```
Syy_eff(ij) = Stress(2,:);  
Txy_eff(ij) = Stress(3,:);  
end  
% END OF Plasticity.m
```

